

Processing and characterization of epitaxial GaAs radiation detectors

X. Wu^{a,*}, T. Peltola^{b,**}, T. Arsenovich^b, A. Gädda^a, J. Härkönen^b, A. Junkes^c, A. Karadzhinova^b, P. Kostamo^d, H. Lipsanen^e, P. Luukka^b, M. Mattila^e, S. Nenonen^d, T. Riekkinen^a, E. Tuominen^b, A. Winkler^b

^aVTT, Microsystems and Nanoelectronics, Tietotie 3, Espoo, P.O. Box 1000, FI-02044 VTT, Finland

^bHelsinki Institute of Physics, P.O. Box 64 (Gustaf Hällströmin katu 2) FI-00014 University of Helsinki, Finland

^cInstitute for Experimental Physics, University of Hamburg, Germany

^dOxford Instruments Analytical Oy, Tarvonsalmenkatu 17, Espoo, Finland

^eAalto University, Department of Micro and Nanosciences, Tietotie 3, Espoo, P.O. Box 13500, FI-02015, Finland

Abstract

GaAs devices have relatively high atomic numbers ($Z=31, 33$) and thus extend the X-ray absorption edge beyond that of Si ($Z=14$) devices. In this study, radiation detectors were processed on GaAs substrates with $110\ \mu\text{m} - 130\ \mu\text{m}$ thick epitaxial absorption volume. Thick undoped and heavily doped p^+ epitaxial layers were grown using a custom-made horizontal Chloride Vapor Phase Epitaxy (CVPE) reactor, the growth rate of which was about $10\ \mu\text{m}/\text{h}$. The GaAs $p^+/i/n^+$ detectors were characterized by Capacitance Voltage (CV), Current Voltage (IV), Transient Current Technique (TCT) and Deep Level Transient Spectroscopy (DLTS) measurements. The full depletion voltage (V_{fd}) of the detectors with $110\ \mu\text{m}$ epi-layer thickness is in the range of $8\ \text{V} - 15\ \text{V}$ and the leakage current density is about $10\ \text{nA}/\text{cm}^2$. The signal transit time determined by TCT is about $5\ \text{ns}$ when the bias voltage is well above the value that produces the peak saturation drift velocity of electrons in GaAs at a given thickness. Numerical simulations with an appropriate defect model agree with the experimental results.

Keywords: GaAs; Solid state radiation detectors; Wafer processing; Defect characterization; TCAD simulations

1. Introduction

Radiation detectors made on epitaxial GaAs are a promising alternative for the silicon devices used for spectroscopy and radiography applications requiring moderate photon energies, i.e. more than $10\ \text{keV}$. Mammography is an important example of such an application with large technological and societal impact. Earlier studies on using GaAs material for X-ray registration include References [1, 2]. The atomic numbers of GaAs are 31 (Ga) and 33 (As) while the atomic number for Si is 14. As a result, for a low energy X-ray process with a photon energy of $20\ \text{keV}$, the mass attenuation coefficients (μ/ρ) are 42.3 and $4.4\ \text{cm}^2/\text{g}$ for GaAs and Si, respectively. The benefit of GaAs is well illustrated

in figure 1. Here, the total absorption efficiency of $20\ \text{keV}$ photons, calculated by Beer-Lambert law, is shown as the function of detector thickness.

As seen in figure 1, the GaAs thickness of $100\ \mu\text{m}$ is enough to absorb about 90% of the $20\ \text{keV}$ photons, while the absorption efficiency of $300\ \mu\text{m}$ thick Si would be only about 27%.

Being the basic starting material in optoelectronics industry, the processing technology of GaAs devices is well established. The epitaxy based on ultra-pure gaseous precursors is a pronounced approach to fabricate pin-diode structured GaAs radiation detectors. When illuminated by X-rays, a GaAs detector operates under the condition of moderate injection level, i.e. the carrier concentration is about $10^{17}\ \text{cm}^{-3}$ [3]. According to the well-known transferred electron effect [4, 5, 6] (further described in section 4), the drift velocity of charge carriers in GaAs decreases after the electric field inside the material has reached the value of about $3.3\ \text{kV}/\text{cm}$ [4].

*Corresponding author

**Speaker, Corresponding author

Email addresses: Xiaopeng.Wu@vtt.fi (X. Wu), timo.peltola@helsinki.fi (T. Peltola)

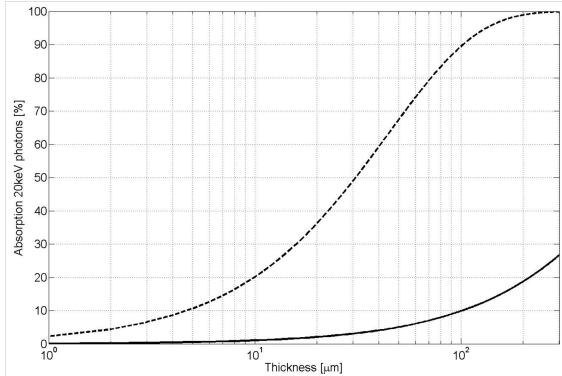


Figure 1: Absorption efficiency vs. detector thickness calculated by Beer-Lambert law. Dashed and solid curves represent GaAs and silicon, respectively.

In a 100 μm thick GaAs detector, this saturation drift velocity of charge carriers would take place when the value of reverse bias is 33 V. The relatively low full depletion voltage (V_{fd}) of GaAs defines the maximum doping concentration to be about $5 \times 10^{11} \text{ cm}^{-3}$. This is challenging to achieve in GaAs crystals manufactured using the bulk growth methods.

A number of deposition techniques have been developed for high purity GaAs epitaxy. Many of these epitaxial growth techniques, however, suffer from high cost, low growth rate or incapability to grow thick layers. On the other hand, chloride vapor phase epitaxy (CVPE) technique has been proved to grow high purity epi-GaAs with a high growth rate (about 10 $\mu\text{m}/\text{hour}$) and with an achievable layer thickness of more than 100 μm , as is required in detector applications. In the following, we present the processing, the results of characterization and the device simulations of the 110 μm thick epitaxial pin-diode GaAs radiation detectors.

2. Processing and design of detectors

Two 2-inch diameter GaAs wafers with CVPE grown intrinsic epitaxial layers were processed to radiation detectors at Micronova nanofabrication center cleanroom. The wafers used in the study were produced by A. F. Ioffe Physico-Technical Institute (Ioffe PTI) [7]. The n-type 460 μm thick epitaxial GaAs wafers were doped with silicon which had a concentration of about 10^{19} cm^{-3} . Undoped epitaxial layers, of thicknesses 110 μm and 130 μm , were grown on the substrates in a horizontal CVPE reactor at 730-760 $^{\circ}\text{C}$ temperatures. Epitaxy was

finalized by the deposition of a 1-2 μm thick zinc doped p^+ layer on the undoped layer to complete the desired p-i-n structure.

After the epitaxy, the wafers were cleaned with acetone and isopropanol to remove particles and possible organic contamination from the surfaces. Mesa structures shown in figure 2 were formed by deep reactive ion etching (DRIE) with BCl₃ plasma. The trench depth was roughly 7 μm in order to ensure sufficient isolation through p^+ region between the segmented region. After etching, a plasma enhanced chemical vapor deposition (PECVD) grown dielectric layer was deposited for surface protection. Openings for contacts to PECVD dielectric were done by wet etching with diluted buffered hydrofluoric acid (BHF). The contact metallization was made by sputtered Ni/TiW/Ni (20 nm/20 nm/40 nm) stacked layers and patterning was completed by a lift-off process. The mechanical grinding and polishing were applied to the substrate side leaving a 20 μm heavily doped n-type GaAs layer for the backside metal contact. As the last process step, a 100 nm thick Ni layer was sputtered on the back plane as the backside contact.

The wafer layout contains two pixel sensors compatible with CERN Medipix CMOS read-out ASIC [7, 8] (256×256 pixels with 55 μm pixel pitch), one strip sensor (128 strips with 200 μm pitch) and several pad diodes (diameter of 1.75 mm). First results of the fabricated GaAs flip-chip bonded pixel devices and their response to X-ray illumination has been reported in Reference [9]. In this report, we focus on diodes, of which design and dimensions are shown in figure 2.

3. Characterization

3.1. CV and IV results

The pad detectors and test structures were characterized by Capacitance Voltage (CV) / Current Voltage (IV), Transient Current Technique (TCT) [10] and Deep Level Transient Spectroscopy (DLTS) measurements. The full depletion voltage (V_{fd}) of the detectors is about 10 V and the leakage current at V_{fd} was in most of the devices below 10 nA/cm². Some of the devices showed breakdown before the V_{fd} . Illustrative examples of CV and IV curves are shown in figures 3 and 4.

The CV measurements were done at room temperature at a frequency of 10 kHz. This was deemed sufficient since the low level of the leakage current

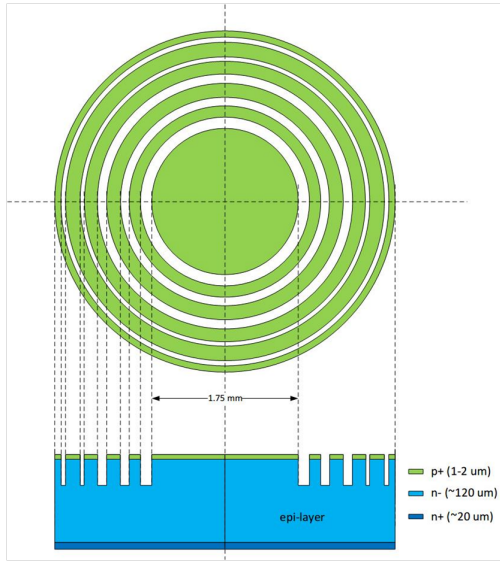


Figure 2: Cross section and design of GaAs pin-diode.

density rules out the possibility of distortion from the generation current of the deep defect levels to the CV results. It can be seen in figure 3 that the GaAs diodes do not show sharp capacitance saturation, which is often the case in e.g. planar silicon pad detectors. This is most likely due to non-abrupt backplane of the pin-diode. The epitaxial deposition at about $760\text{ }^{\circ}\text{C}$ of $>100\text{ }\mu\text{m}$ thickness takes more than ten hours. It is comprehensible that diffusion from heavily doped substrate takes place in some extent, resulting in a non-abrupt $i\text{-}n^+$ transition region that is observed by non-saturated CV characteristics. The leakage currents in the devices were typically $100\text{-}200\text{ pA}$, corresponding to the current density of about 10 nA/cm^2 . The leakage current tends to saturate after the V_{fd} and breakdown occurs in good devices after about 200 V , i.e. over ten times higher voltage than the V_{fd} . More statistics of the leakage current has previously been reported in Reference [9].

3.2. TCT results

Transient current technique (TCT) measurements were performed at the premises of Detector Laboratory of Helsinki Institute of Physics (HIP). The detectors were assembled on a PCB substrate by a conductive silicon carbide tape and a probe needle. Optical excitation was done by a red laser (678 nm) emitting 30 ps (FWHM) pulse to the segmented p^+ side of the diode. Detectors were capacitively decoupled from the 4 GHz oscilloscope

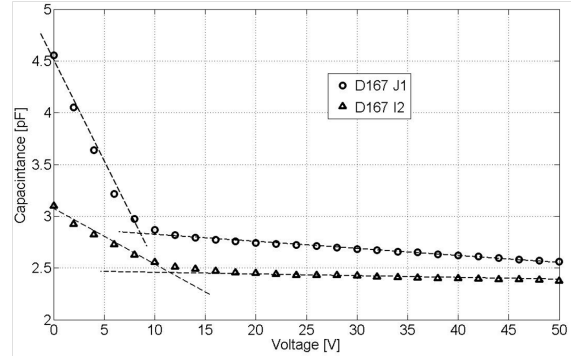


Figure 3: CV curves of the two ($110\text{ }\mu\text{m}$ thick i -layer) GaAs pad detectors. Geometrical capacitance calculated from the surface area in figure 2 is $\sim 2.32\text{ pF}$. The minimum capacitances indicate about 9% smaller active thickness for the D167 J1 diode. Full depletion voltages of $\sim 8.5\text{ V}$ and $\sim 12\text{ V}$ for the D167 J1 and D167 I2, respectively, were determined from the crossing points of the linear fits.

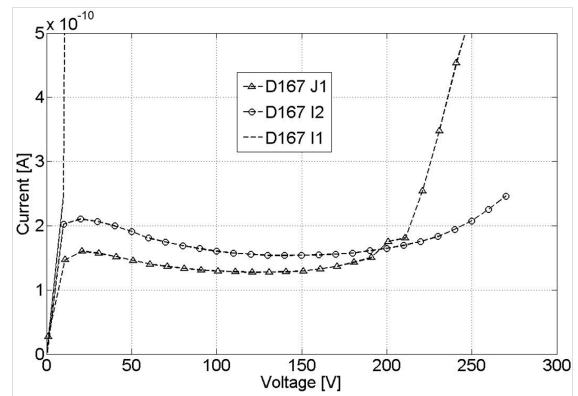


Figure 4: Current Voltage curves of two ($110\text{ }\mu\text{m}$ thick i -layer) GaAs pad detectors.

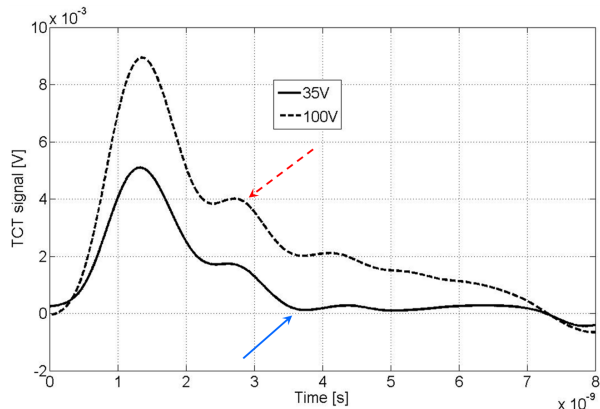


Figure 5: TCT measurement for GaAs diode biased with 35 V and 100 V.

by Miteq Ltd. Bias-T and the signal was amplified by a broad band amplifier provided by Particulars Ltd. Since the absorption depth of 678 nm light in GaAs is less than $1 \mu\text{m}$, the holes excited by the incident photons will be inherently quickly collected by the adjacent p^+ -electrode and the current transient observed by the oscilloscope is the current created by the electrons drifting the entire thickness of the pin-diode. Since the epi-layer is n^{--} type, the electrons are majority carriers (not minority) and their radiative lifetime can be ignored. In high purity, high quality GaAs the radiative lifetime can be very long, even in the microsecond regime [11].

The curves shown in figure 5 are the electron current transients at 35 V and 100 V bias voltages. The duration of the transient is about 5 ns when biased with 100 V. The electron current transient time at 35 V bias is clearly shorter, about 3.5 ns, than at 100 V indicating higher drift velocity in case of lower electric field. The parasitic oscillations after the second peak in both of the curves were not considered as a part of the signal. Thus, for the collection time estimation the slope of the 100 V curve was extrapolated to zero after the second peak (indicated by a red dashed arrow in the figure) and the duration of the 35 V curve was determined from the location indicated by a blue arrow. In this particular measurement, the laser spot was not collimated. Thus, there is discrepancy in integrated collected charge due to the charge flow in lateral direction.

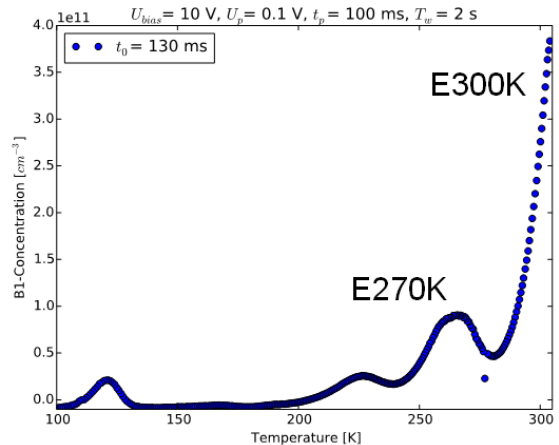


Figure 6: DLTS measurement with electron injection. U_{bias} is the reverse bias voltage, U_p is the forward pulse voltage, t_p is the pulse time, T_w is the acquisition time window and t_0 data recording cut.

3.3. DLTS results

The Deep Level Transient Spectroscopy (DLTS) analysis for GaAs diodes was performed at University Hamburg. The DLTS spectra of electron and hole injections are shown in figures 6 and 7, respectively. The analysis shows two deep electron traps peaking at $T = 270 \text{ K}$ (E270) and $T \geq 300 \text{ K}$ (E300). Due to the technical restrictions, it was not possible to unambiguously define the electrical properties and concentration of E300 trap. The hole traps were observed at low temperatures, therefore they appear to be shallow defects, with concentrations of a few 10^{10} cm^{-3} . A contribution of such shallow defects to the leakage current is very unlikely. It is more apparent that deep defects contribute in GaAs pin-diodes. The deeper defects found in the DLTS spectra are better candidates for dominating the current. DLTS measurements up to 450 K have to be performed to check the existence of the very deep defects.

4. TCAD simulations and modeling

The simulations presented in this paper were carried out using the Synopsys Sentaurus¹ finite-element Technology Computer-Aided Design (TCAD) software framework.

¹<http://www.synopsys.com>

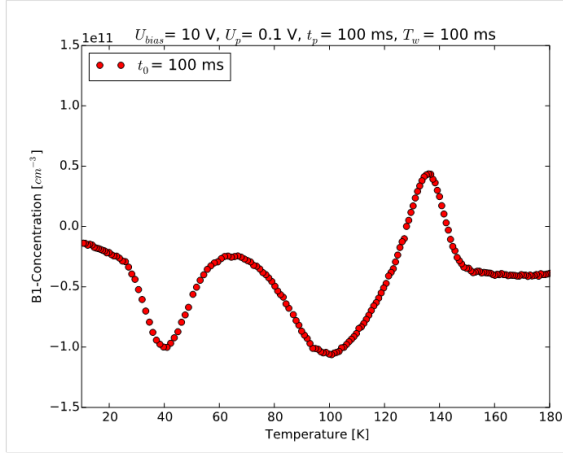


Figure 7: DLTS measurement with hole injection.

4.1. GaAs diode parameters and CV/IV results

The initial simulated GaAs diode structure had the dimensions $A \times 10 \times 131.5 \mu\text{m}^3$, where A is the area factor to match the dimensions with the diode in figure 2. The thicknesses of the DC-coupled nickel contacts on the front and backplanes were 100 nm. Presented in figure 8, the heavily doped p^+ and n^+ implantations on the front and backplane, respectively, had the peak concentrations $1 \times 10^{19} \text{cm}^{-3}$. The doping profiles were tuned to create approximations of the layer thicknesses presented in section 2. The diode was biased by setting the electrode on the front surface to zero potential while the reverse voltage was provided from the backplane contact.

To reproduce the measured geometric capacitances, full depletion voltages and leakage current densities in figures 3 and 4, the deep donor level suggested in section 3.3 was implemented to the GaAs epi-layer. As can be seen from figure 9 the simulated results are in line with the measurements after the capture cross section and concentration were tuned to $\sigma = 5 \times 10^{-10} \text{cm}^2$ and $N_t = 1.4 \times 10^{12} \text{cm}^{-3}$, respectively.

4.2. Transient current simulation results

In GaAs and materials of similar band structure a negative differential mobility is generated by high driving fields. This effect is caused by the transfer of electrons into an energetically higher side valley with a considerably larger effective mass, i.e. when the electric field in the material reaches a threshold level, the mobility of electrons starts to

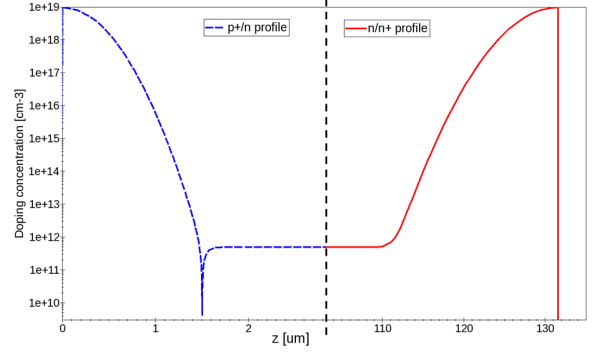


Figure 8: Simulated doping profiles of p^+ and n^+ layers with tuned diffusion depths to create an effective structure similar to the real GaAs diode described in section 2.

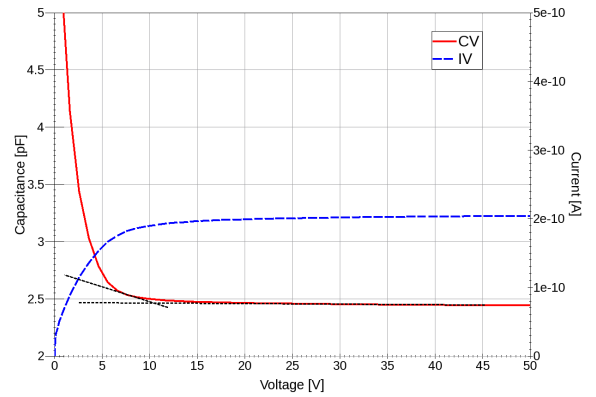


Figure 9: Simulated CV ($f = 10 \text{ kHz}$) and IV curves at $T = 300 \text{ K}$ for the measured GaAs diode parameters in section 2 with an active area thickness of $110 \mu\text{m}$ and with the deep donor level from section 3.3. The geometrical capacitance is $\sim 2.32 \text{ pF}$ while the leakage current density is $\sim 8.5 \text{ nA/cm}^2$. The full depletion voltage of about 10 V was determined as in figure 3.

decrease with increased electric field due to transferred electrons from one valley in the conduction band to another. In the process the electron effective mass moves from small to large and the mobility decreases from very high to very low [4, 5]. For the simulation of the effect the charge injection depth was set to $\sim 3 \mu\text{m}$ from the device front surface to generate the transient signal essentially from the electron drift.

Illustrated in figure 10 are the simulated transient currents in the GaAs diode at $T = 300 \text{ K}$. As can be seen, the macroscopic result of the transferred electron effect is reproduced, i.e. when the voltage and thus, the electric field in the diode moves closer to the values that produce the saturation of the electron drift velocity a reduced collection time t_{coll} is observed. In the GaAs diode with an active volume thickness of about $110 \mu\text{m}$ the voltage required for the saturation is $\sim 37 \text{ V}$. The simulated transient signal shapes and the difference in signal heights are in line with the measurements in figure 5. To reproduce the signal height differences agreeing with the measurement the simple diode structure described in section 4.1 had to be replaced by a larger structure that took into account the lateral expansion of the electric field beyond the diode region. If the lateral expansion of the electric field is not considered the fields for the given voltage will be higher than in the real diode, affecting the drift velocities. For simplicity, the deep donor level was not applied for the transient simulations that were carried out to investigate the transferred electron effect. Hence, the absolute collection times are shorter than the measured.

5. Conclusions

X-ray detectors made on thick epitaxial GaAs were successfully processed at Micronova Nanofabrication Centre. The epitaxial GaAs layers were grown in a horizontal Chloride Vapor Phase Epitaxy (CVPE) reactor. A growth rate of undoped GaAs of about $10 \mu\text{m/h}$ was achieved and pin-diode devices having undoped layer thicknesses of $110 \mu\text{m}$ and $130 \mu\text{m}$ were grown. The finalized detectors were subjected to CV/IV , TCT and DLTS characterization. The full depletion voltage (V_{fd}) is in the range of 8-15 V and the leakage current density in the order of 10 nA/cm^2 . According to the TCT measurements, the signal is collected faster than in 10 ns, while the DLTS analysis revealed a significant

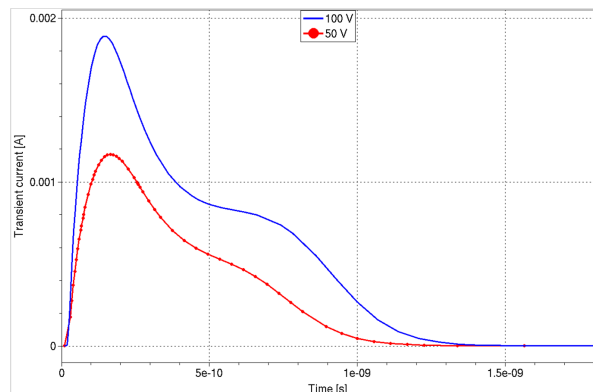


Figure 10: Simulated transferred electron effect on transient current in GaAs diode. The shortest collection time is given by the voltage producing a drift velocity closest to the saturation value.

concentration of deep level electron traps in the epitaxial layer. TCAD simulations with an effective deep donor defect level reproduced the measured leakage current density and full depletion voltage. The transient simulations displayed the transferred electron effect producing similar behaviour with the measured TCT signals.

Thus, it can be concluded that these GaAs sensors are suitable for soft X-ray detection. There is ongoing work with a new vertical CVPE reactor to optimize the epitaxial process in terms of dislocation density as well as to better control the intrinsic stress causing wafer bow.

References

- [1] A. Owens, A. Peacock, Compound semiconductor radiation detectors, Nucl. Instr. & Meth. A 531 (1-2) (2004) 18–37. doi:10.1016/j.nima.2004.05.071.
- [2] P. Sellin, J.Vaitkus, New materials for radiation hard semiconductor detectors, Nucl. Instr. & Meth. A 557 (2) (2006) 479–489. doi:10.1016/j.nima.2005.10.128.
- [3] P. Bhattacharya, Semiconductor Optoelectronic Devices, 2nd Edition, Prentice Hall Inc., 1997.
- [4] J. G. Ruch, G. S. Kino, Transport properties of GaAs, Phys.Rev. 174 (3) (1968) 921–931. URL <http://journals.aps.org/pr/pdf/10.1103/PhysRev.174.921>
- [5] A. Dargys, J. Kundrotas, Handbook on the physical properties of Ge, Si, GaAs and InP, 1st Edition, Science and Encyclopedia Publ., Vilnius, Lithuania, 1994.
- [6] S. M. Sze, Physics of Semiconductor Devices, 2nd Edition, John Wiley & Sons, New Jersey, 1981.
- [7] P. Kostamo, S. Nenonen, S. Vähänen, L. Tlustos, C. Fröjdh, M. Campbell, Y. Zhilyaev, H. Lipsanen, GaAs Medipix2 hybrid pixel detector, Nucl. Instr. & Meth. A 591 (2008) 174–177. doi:10.1016/j.nima.2008.03.050.

- [8] L. Tlustos, M. Campbell, C. Fröjdh, P. Kostamo, S. Nenonen, Characterisation of an epitaxial GaAs/Medipix2 detector using fluorescence photons, Nucl. Instr. & Meth. A 591 (2008) 42–45. doi:10.1016/j.nima.2008.03.020.
- [9] X. Wu, et al., Radiation detectors fabricated on high-purity GaAs epitaxial materials, JINST 9 (C12024). doi:10.1088/1748-0221/9/12/C12024.
- [10] V. Eremin, N. Strokan, E. Verbitskaya, Z. Li, Development of transient current and charge techniques for the measurement of effective net concentration of ionized charges (N_{eff}) in the space charge region of p-n junction detectors, Nucl. Instr. & Meth. A 372 (1996) 388–398. doi:10.1016/0168-9002(95)01295-8.
- [11] R. Dingle, Radiative Lifetimes of Donor-Acceptor Pairs in p-Type Gallium Arsenide, Phys.Rev. 184 (3) (1969) 788–796. doi:10.1103/PhysRev.184.788.